Development mechanism of a cumulonimbus observed by Ka-band Doppler radar on 18 August 2011 in the Kanto region, Japan

Namiko Sakurai[1], Shingo Shimizu[1], Koyuru Iwanami[1], Ryohei Misumi[1],

Shin-ichi Suzuki[1], Takeshi Maesaka[1], Yukari Shusse[1], and Seiichi Shimada[1]

[1]*National Research Institute for Earth Science and Disaster Prevention, Tsukuba, Japan*

1 Introduction

Local severe weather often occurs in the summer season in the Tokyo Metropolitan Area, Japan and causes heavy damage such as flash floods, power failure, and traffic congestion. To mitigate such disasters, it is necessary to develop techniques for the early detection of cumulonimbi that will cause local severe damage and for the high accuracy prediction of local severe weather.

Millimeter-wavelength radar is a useful tool for observing the initiation and early developing stage (DS) of cumulonimbi because it has higher sensitivity and higher spatial resolution than those of conventional weather radars (S-, C-, and X-band radars; centimeter-wavelength radars). However, there are few previous studies of the initiation and development of a cumulonimbus using millimeter-wavelength radar (Kobayashi et al., 2011; Sakurai et al, 2012). The National Research Institute for Earth Science and Disaster Prevention (NIED) of Japan has a Ka-band Doppler radar (KaDR) with mobile capability (Iwanami et al., 2001) and performed intensive observation of cumulonimbi with the KaDR and an X-band polarimetric Doppler radar (MP-X) in the western Kanto region, Japan during the summer of 2011-2013 (Fig. 1). Sakurai et al. (2012) successfully observed a cloud from initiation to the DS using the KaDR and from the DS to the dissipation stage using the MP-X on 18 August 2011. On the morning of this day, the cumulonimbus emerged in the mountainous western part of Kanto region and produced maximum rainfall amount of 29 mm. From the analysis of the KaDR and MP-X data, three characteristics of the initiation and development process of the cumulonimbus were described in their paper.

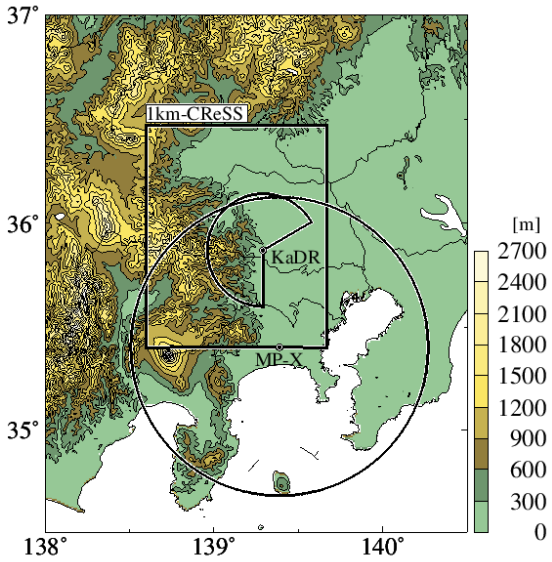

Figure 1: Observation area and simulation domain of 1km-CReSS. Ka-band Doppler radar (KaDR) was installed at Hidaka City, Japan and X-band polarimetric Doppler radar (MP-X) was installed at Ebina City, Japan. Contours and shade show topography height.

1. The echo top height and maximum reflectivity developed in three steps, and gradual development of the echo top height with three steps corresponded to the height of stable layers in the atmosphere. In the beginning of the DS, convection was shallow (~5 km ASL) with weak reflectivity value. The MP-X could not detect any cumulonimbus echo in the beginning of the DS. It should be noted that the minimum detectable intensity of the KaDR (MP-X) was -16.4 dBZ (about 20 km) (11.9 dBZ (about 60 km)). In the middle of the DS, the echo top height and reflectivity increased, and the MP-X first detected an echo. In the end of the DS, echo top height and reflectivity became higher than those in the middle of the DS. The maximum echo top height exceeded 12 km ASL in the end of the DS. Thus, the following convective activity broke through the stable layers in the middle of the DS, and echo top height finally reached 12 km ASL in the end of the DS.
2. Sakurai et al. (2012) found misoscale convective echoes which appeared to the side of pre-existing echoes and developed vertically and/or spatially. The misoscale convective echoes which were newly detected in an RHI and PPI scan and developed vertically (RHI scan) or spatially (PPI scan) were labeled as a ‘new misoscale convective echo’ (NMCE). The time lag between the detection of NMCEs by the KaDR and the MP-X became smaller as the cumulonimbus developed.
3. The NMCE was concentrated in two height regions. In the first half of the DS, the NMCE was observed between 2 and 5 km ASL; however, the NMCE was observed between 5 and 12 km ASL in the second half of the DS. The NMCE height corresponded to the height of stable layers. However, the reason why the NMCE height is related to that of a stable layer is unknown.

To clarify the development mechanism of the cumulonimbus described by Sakurai et al., (2012), we tried to reproduce the process of initiation and development of the cumulonimbus using a Cloud Resolving Storm Simulator (CReSS; Tsuboki and Sakakibara, 2002).

 sakurain@bosai.go.jp

2 Numerical model setting

To clarify the development mechanism of the cumulonimbi, we performed numerical simulations using a CReSS, which is a 3D non- hydrostatic model developed by the Hydrospheric Atmospheric Research Center (HyARC) of Nagoya University, Japan (Tsuboki and Sakakibara, 2002). This model employs fully compressible, non-hydrostatic dynamics, and is designed to realistically simulate mesoscale systems, at high resolution, using explicit cloud microphysical scheme (see Table 1 for a detailed description of the model). CReSS adopts a terrain-following curvilinear coordinate in the vertical. With this coordinate system, the equations for 3D momentum, pressure, and potential temperature (θ) are formulated as described in detail by Tsuboki and Sakakibara (2002). The predicted variables are the 3D wind components (u, v, and w), the pressure and potential temperature perturbations (p´ and θ´) from the mean state, which is in hydrostatic equilibrium at the starting time of model integration.

The CReSS model includes a two moment bulk cold-rain parameterization and a 1.5-order closure with a turbulent kinematic energy prediction (Tsuboki and Sakakibara, 2001). The prognostic variables in microphysics are the mixing ratios of water vapor (q_v), cloud water (q_c), rain (q_r), cloud ice (q_i), snow (q_s), and graupel (q_g), and the number concentrations of cloud water (N_c), rain (N_r), cloud ice (N_i), snow (N_s), and graupel (N_g). The microphysical principles incorporated into CReSS are based on Lin et al. (1983), Cotton et al. (1986), Murakami (1990), Ikawa and Saito (1991), and Murakami et al. (1994).

The domain of the CReSS simulation is shown in Fig. 1. The horizontal domain had 120 × 120 grid points, with a time step of $\Delta t = 1$ s. During the simulation, the horizontal grid size was 1 km, and the vertical grid contained 80 levels with variable grid intervals ($\Delta z = 100$ m below 5 km in height, and Δz was gradually stretched up to about 800 m above 5 km). First of all, we ran CReSS with a full physical model containing topography using Japan Meteolorogical Agency Meso Spectral Model (JMA MSM) or JMA Mesoscale Analysis (MA) for the initial and lateral boundary conditions of the numerical simulations. However, this experiment did not reproduce the cumulonimbus. Therefore, we assimilated GPS precipitable water data obtained near the initiation area of convection to improve the initial condition. However, the simulated precipitation amount was overestimated, and gradual development of the cumulonimbus was not reproduced: the simulated cumulonimbus developed sharply. This failure may result from the absence of stable layers due to its coarse vertical resolution, which contributed to gradual development of the cumulonimbus, in the MSM/MA data. Therefore, we performed the following three numerical simulations to reproduce the development process of the present cumulonimbus. We used sounding data at Tateno at 09 JST (JST = UTC + 9 hr) on 18 August 2011 for the initial and lateral boundary conditions. First, for the control experiment (CNTL), we ran CReSS with a full physical model containing topography. Second, we ran an experiment that positive perturbation of θ (3 K) was added continuously as a buoyancy forcing at a height of 500 m around initiation region of the convection observed by the KaDR (CONT experiment). Third, we ran an experiment similar to the CONT experiment except that intermittent forcing of θ was given with an interval of 15 minutes (INTM experiment).

Table 1:Specifications of CReSS.

Model feature	Description
Basic equation	Quasi-compresible nonhydrostatic Navier-Stokes equation with a map factor
Projection	Lambert conformal conic
Vertical coordinate	Terrain-following
Grid	Staggered Arakawa C type in the horizontal and Lorenz type in the vertical
Advection scheme	Antiflux form with fourth-order central differential
Diffusion scheme	Fourth-order differential method
Turbulent closure	1.5-order closure scheme
Time splitting	Horizontal explicit and vertically implicit for sound waves
Precipitation scheme	Bulk tow moment cold-rain scheme (predicting q_v, q_c, q_r, q_i, q_s, q_g, N_c, N_r, N_i, N_s, and N_g)
Surface layer	Bulk method similar to Segami et al. (1989)
Lower boundary	Rigid; temperature is forecast using a 30-layer one-dimensional model
Upper boundary	Rigid lid with absorbing layer
Lateral boundary	Radiative boundary condition

3 Results

In the CNTL experiment, convection did not emerge and the cumulonimbus was not reproduced in the mountainous area (figure not shown). In the CONT experiment, a convection emerged in the mountainous area soon after the start of the simulation and the convection became deep sharply. In this simulation, gradual development of the cumulonimbus was not reproduced, which is not consistent with the behavior of the cumulonimbus observed by the KaDR and the MP-X (figure not shown).

In the INTM experiment, several convections emerged in the mountainous area during 0900-1200 JST. Time variations of echo top height of two convections which developed up to upper troposphere were shown in Fig. 2. These two convections migrated eastward due to advection by back-ground westerly wind (figure not shown). The latter convection developed deeper than the former one, which is consistent with an observation result (Sakurai et al., 2012). The former convection emerged at a height of around 2 km at 0919 JST, and the convection was shallow until 0932 JST. The convection started developing gradually from 0933 to 1025 JST up to 10.0 km in height. In the DS of the former convection, the development was suppressed during 1003 and 1006, and 1016 and 1018 JST at a height of 5.4 and 8.4 km, respectively. The suppression height corresponds to the height of stable layers (right panel of Fig. 2). The latter convection emerged at a height of around 2 km at 1005 JST and developed up to 17.2 km in height. Similar to the former convection, this latter convection was also suppressed at a height of 5.4, 8.0, 10.1, 13.5, 14.1, 15.6, and 16.4 km. In this experiment, gradual development of the cumulonimbus associated with stable layers was reproduced well.

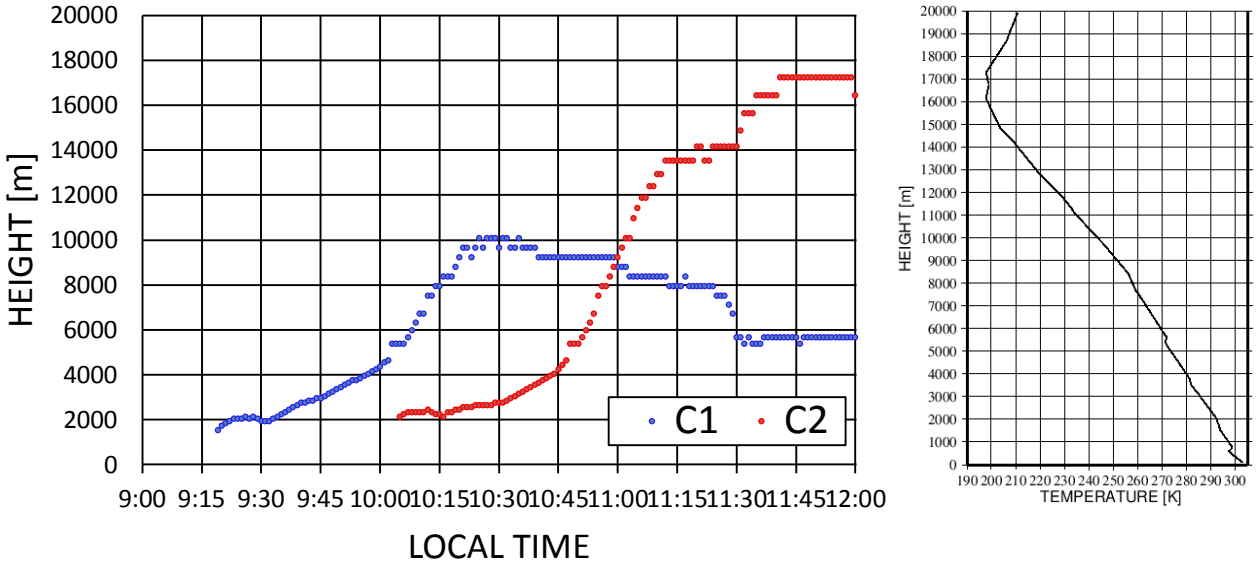

Figure 2: Left panel shows temporal variations of echo top height simulated in the INTM experiment. Two convections were traced and those of echo top height ware plotted (C1 and C2). Right panel shows sounding profile of temperature observed at Tateno at 0900 JST on 18 August 2011.

4 Summary

We tried to reproduce gradual development of the cumulonimbus observed by the KaDR and the MP-X on 18 August 2011 using the CReSS. In the CNTL experiment, no convection was reproduced. In the CONT experiment, the convection emerged but a cumulonimbus developed sharply, which means that the observed cumulonimbus was not reproduced. In the INTM experiment, gradual development of the cumulonimbus was reproduced: in the beginning of the DS, convection was shallow for several minutes and the convection developed gradually. The development of the convection was suppressed around stable layers. The latter convection developed deeper than the former one, which is also consistent with observational result.

In this study, we added intermittent forcing of θ with an interval of 15 minutes and could reproduce the cumulonimbus development observed by the KaDR and the MP-X on 18 August 2011. To give a reasonable meaning of the intermittent forcing will be left as a future work. The following points remains as future works to reproduce the cumulonimbus development more accurately.

1. In the beginning of DS, more shallow convections were observed than simulation results in the INTM experiment (Fig. 4 in Sakurai et al., 2012). In the INTM experiment, a few shallow convections were reproduced. One possibility of this problem is coarse spatial resolution of numerical simulation. We will try to simulate the cumulonimbus with higher spatial resolution than the present setting (1 km).
2. It is impossible to reproduce NMCEs in the setting of the present numerical simulation. Because the horizontal scale of NMCE was several hundred meters. The experiment with higher spatial resolution is needed to reproduce NMCEs.

After we succeed in reproducing the cumulonimbus in more accurately, we will investigate the role of shallow preceding convection for the development of following convection and the reason why the time lag between the detection of NMCEs by the KaDR and the MP-X became smaller as the cumulonimbus developed.

References

Braham Jr., R., 1958: Cumulus cloud precipitation as revealed by radar –Arizona 1955. *J. Meteor.*, 15, 75-83.

Cotton W.R., G.J. Tripoli, R.M. Rauber, E.A. Mulvihill, 1986: Numerical simulation of the effects of varying ice crystal nucleation rates and aggregation processes on orographic snoufall. *J. Climate Appl.*, 25, 1658-1680.

Horie, H., and K. Tomine, 1998: A study of generation and movement of air mass thundersorms over Kanto area in summer 1995. *Tenki*, 45, 441-453 (in Japanese).

Ikawa, M., and K. Saito, 1991: Description of a nonhydrostatic model developed at the forecast research department of the MRI. *MRI Tech. Rep.*, 28, Meteorological Research Institute 238 pp ([Available online at http://www.mri-jma.go.jp/Publish/Technical/DATA/VOL_28/28_en.html])

Iwanami, K., R. Misumi, M. Maki, T. Wakayama, K. Hata, and S. Watanabe 2001: Development of a multiparameter radar system on mobile platform. *Proc. 30th Conf. on Radar Meteor.*, 104-106.

Iwanami, K., Y., Chono, T. Harimaya, J. Testud, M. Maki, R. Misumi, and S.-G. Park 2005: Retrieval of vertical rain rate profile by dual-frequency radar data. *Proc. 32th Conf. on Radar Meteor.*, 104-106.

Kobayashi, F., and N. Inatomi, 2003: First radar echoformation of summer thunderclouds in southern Kanto, Japan. *J. Atmos. Electricity*, 23, 9-19.

Kobayashi, F., T. Takano, and T. Takamura, 2011: Isolated cumulonimbus initiation observed by 95-GHz FM-CW radar, X-band radar, and photogrammetry in the Kanto region, Japan. *SOLA*, 7, 125-128.

Lin, Y.-L., R.D. Farley, and H.D. Orville, 1983: Bulk parameterization of te snow field in a cloud model. *J. Appl. Meteor.*, 22, 1065-1092

Maesaka, T., M. Maki, K. Iwanami, S. Tsuchiya, K. Kieda, and A. Hoshi, 2011: Operational rainfall estimation by X-band MP radar network in MLIT, Japan. *Proc. 35th Conf. on Radar Meteor.*, 12-18.

Murakami, M., 1990: Numerical modeling of dynamical and microphysical evolution of an isolated convective cloud-the 19 July 1981 CCOPE cloud. *J. Meteor. Soc. Jpn*, 68, 107-128

Murakami, M., T.L. Clark, W.D. Hall, 1994: Numerical simulations of convective snow clouds over the sea of Japan: Two-dimensional simulations of mixed layer development and convective snow cloud formation. *J. Meteor. Soc. Jpn*, 68, 43-62.

Nodzu, M., S. Ogino, Y. Tachibana, and M. D. Yamanaka, 2006: Climatological description of seasonal variations in lower-tropospheric temperature inversion layers over the Indochina peninsula. *J. Climate*, 19, 3307-3319.

Ohno, H., 2001: Thundersorm and meso scale meteorology. *TOKYODOSHOTEN*, 309pp (in Japanese).

Sakurai, N., K. Iwanami, T. Maesaka, S. Suzuki, S. Shimizu, R. Misumi, D.-S. Kim, and M. Maki, 2012: Case study of misoscale convective echo behaviour associated with cumulonimbus development observed by Ka-band Doppler radar in the Kanto region, Japan. *SOLA*, 8, 107-110.

Segami, A., K. Kurihara, H. Nakamura, M. Ueno, I. Takano, and Y. Tatsumi, 1989: Operational mesoscale weather prediction with Japan Spectral Model. *J. Meteor. Soc. Jpn*, 67, 907-924.

Tsuboki, K., and A. Sakakibara, 2001: CReSS User's Guide, 2nd ed. 210 ([available from http://www.rain.hyarc.nagoya-u.ac.jp/~tsuboki/cress_html/src_cress/CReSS2223_users_guide_eng.pdf].

Tsuboki, K., and A. Sakakibara, 2002: Large-scale parallel computing of cloud resolving storm simulator. High Performance Computing. In: Zima, H.P., et al. (Ed.), Proceedings of the Fourth International Symposium on High Performance Computing. Springer, pp.243-259.